- To study the role of nanoparticles in tribological contexts and understand the mechanism of friction and wear.
- To find out the optimum tribological performance of nanoparticles (i.e., the optimum dose of nanoparticles) in the different grades of PAO oil.
- To explore the dispersion stability of nanoparticles in all PAO grades.
- To optimize the various control parameters by using the Taguchi method to assess the tribological properties of PAOs based nanolubricants
- To explore PAO 100 as a base oil and lithium soap as a thickener for the formulation of greases and examine their physicochemical and tribological performance.

2.10. Justification for selection of different nanoparticles

It is reported that MWCNTs as lubricant additives are effective in many tribological applications by their unique architecture (tubular), high flexural and tensile strengths, high elastic modulus, and excellent thermal properties. The superior mechanical properties and the tubular shape of MWCNTs enable them to sustain high loads in tribological applications. Moreover, hollow-core carbon nanotubes offer slippery as well as rotating action relative to each other. Because of such actions, MWCNTs form close to optimal nano-bearings. LaF_3 nanoparticles were selected because they exhibit relatively low hardness, hexagonal crystal allotrope, high melting point, and good thermal and chemical resistance. Also, LaF_3 nanoparticles have been used as extreme pressure and anti-wear additive in greases and lubricating oil.

2.11. Summary of the chapter

This chapter provides an in-depth understanding of PAO oils, additives, nanolubricants, and their tribological behaviour based on previous research work. The gap in nanolubricants tribology was assessed and consequently defined the objective of the work.

Chapter-3

Blank page

3. Materials and Experimentation details

This chapter provides the details of materials used, synthesis of nanoparticles, and grease. A brief description of experimental procedures used in the present work is highlighted. Furthermore, a quick overview of the various analytical techniques employed to analyse nanoparticles and worn surfaces is also described.

3.1. Materials

3.1.1. Base oils

The current study aims to develop synthetic-based nanolubricants (i.e., group IV lubricants) for industrial and automotive applications. Therefore, for the comparative analysis, the different grades of PAOs (i.e., PAO 4, PAO 6, PAO 40, and PAO 100) and polypropylene glycol (PPG 2000) were selected as the base oil for experimentation. The PAO 4 was purchased from Aero Biotechnique, New Delhi, India, and PAO 6, PAO 40, PAO 100, and PPG 2000 were procured from Synthomaxx India Pvt. Ltd., Vapi, India. The typical characteristics of all the base oils are listed in **Table 3.1**.

3.1.2. Lubricant additive

Two types of lubricant additive with a minimal range of concentration (i.e., 0.025-0.15 wt.%) were used in the present study are as follows:

3.1.2.1. COOH-functionalized multiwalled carbon nanotubes (MWCNTs)

The commercially available COOH-functionalized MWCNTs were procured from Otto Chemie Pvt. Ltd., Mumbai, India, as lubricant additives to prepare nanolubricants. As per the manufacturer's data, the properties of additives are presented in **Table 3.2**.

Table 3.1: Physical attributes of different base oils (Supplier's data)

Property	ASTM standards	PAO 4	PAO 6	PAO 40	PAO 100	PPG 2000
Kinematic viscosity (cSt @ 100°C),	D445	4.1	5.8	39	100	24
Kinematic viscosity (cSt @ 40°C),	D445	19	31	396	1150	160
Viscosity index	D2270	126	138	147	179	182
Density (g/mL)	D1298	0.821	0.827	0.850	0.853	1.002
Pour point (°C)	D97	-66	-57	-36	-30	-30
Flash point (°C),	D92	220	246	281	300	229
Noack volatility (wt.%)	D5800	14	6.4	0.7	0.6	-

Table 3.2: Properties of MWCNTs (Supplier's data)

Peculiarity of MWCNTs	Typical value/range
Appearance (form/colour)	Powder/Black
Morphology	Tubular
Accuracy	99%
Outer diameter (nm)	20-30
Length (μm)	1-2
Specific Surface Area (SSA, m^2/g)	130-180
Density (g/cm^3)	0.8-1.8
Young modulus (TPa)	1.7-2.4

3.1.2.2. Oleic acid-modified lanthanum trifluoride (LaF_3) nanoparticles

The oleic acid-modified LaF_3 nanoparticles were synthesized in the laboratory. Different chemicals (analytical grade) were used to synthesize the nanoparticles and are listed in **Table 3.3**.

Table 3.3: List of the analytical grade chemicals used in the preparation of LaF_3 nanoparticles

Chemical name	Chemical formulae	Used for	Manufactures
Ammonium fluoride	NH_4F	Synthesis	SRL Chemicals, India
Lanthanum chloride	$Lacl_3$	Synthesis	Avra Chemicals, India
Oleic acid	$C_{18}H_{34}O_2$	Modification	SD-fine Chemicals, India
Petroleum ether	C_6H_{14}	Modification	SD-fine Chemicals, India
Ethanol	C_2H_6O	Synthesis	CH-fine chemicals, China
Distilled water	H_2O	Synthesis	-

- **The synthesis of LaF_3 nanoparticles**

The LaF_3 nanoparticles were synthesized by the sol-gel method [94] and modified with oleic acid. **Figure 3.1** depicts the synthesis procedure of LaF_3 nanoparticles. A 100 mL solution of NH_4F-ethanol-water (0.45 M) was dissolved into a 100 mL solution of $Lacl_3$-ethanol-water (0.3M) through vigorous stirring for 2 hours. After two hours of reaction of mixtures under stirring, the transparent solution was transformed into a white emulation solution. Then, a mixture of oleic acid (0.045 M) and 100 ml petroleum ether was blended into a white emulsion solution for a reaction period of 1 hour. After that, the reaction mixture was stored for 1 hour for ethanol-water separation. Finally, the upper white phase of the reaction mixture was collected and sequentially washed and centrifuged with ethanol several times to remove the remaining impurities, followed by drying at 70°C in a hot air oven for 12 hours. The resultant white powder was the oleic acid-modified LaF_3 (OA-LaF_3) nanoparticles.

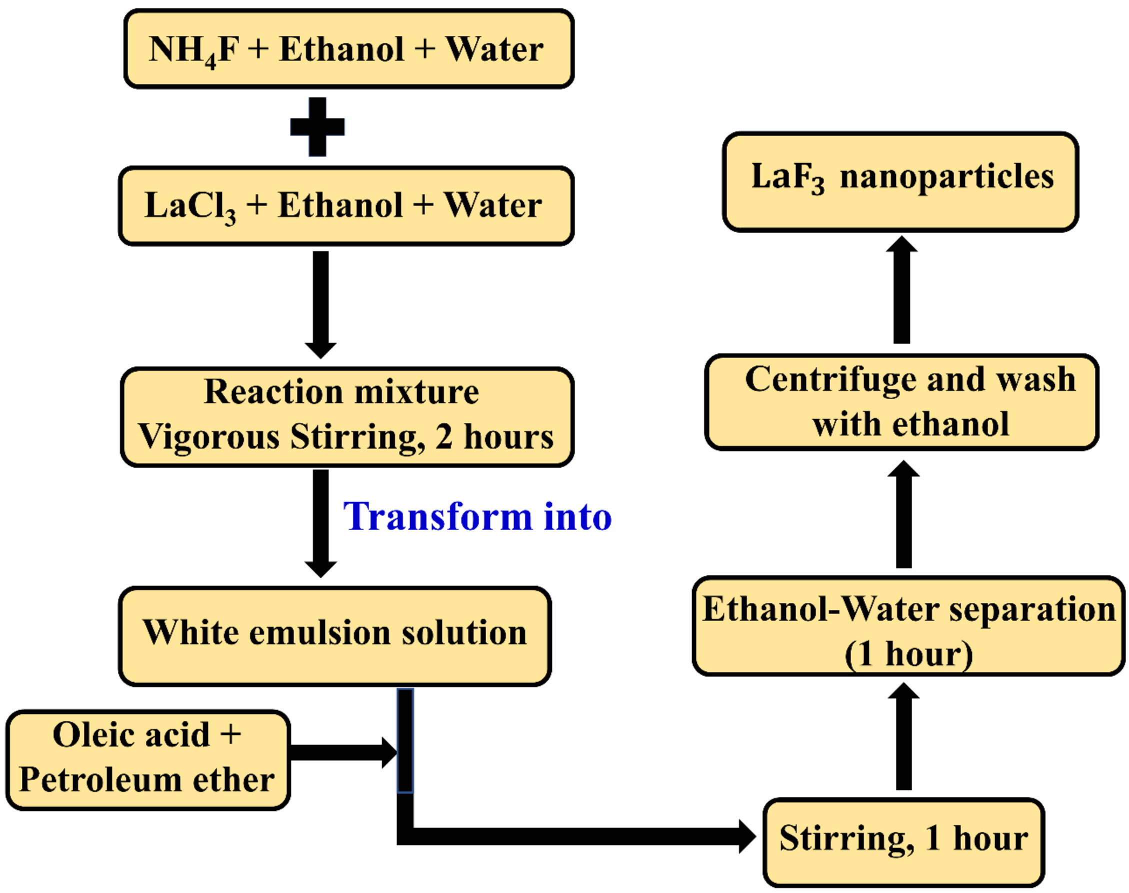

Figure 3.1: Synthesis methodology of LaF_3 nanoparticles

3.2. Characterization of nanoadditives

3.2.1. Transmission electron microscope (TEM)

A high-resolution transmission electron microscope (HR-TEM; Tecnai G2; FEI, Hillsboro, OR) was used to perform the morphological and nanostructure analysis of nanoadditives. For sample preparation, the ethanolic dispersion of each nanoadditive was drop–cast on a separate TEM grid (ϕ–3 mm, thickness 100 µm, and 200 mesh lacey carbon). A high vacuum in the range of 10^{-6} Torr was required to acquire low and high–resolution TEM images.

3.2.2. X-ray diffractometer (XRD)

The X-ray diffractometer (XRD, Rigaku miniflex, USA) with Cu–Kα radiation having a wavelength of 1.54 A° was performed in the range 10° - 90° to identify the crystalline phase and lattice structure nanoadditives. X-ray beams incident on powder or thin-film samples will be diffracted because of crystallographic planes. The distribution of the scattering from the sample reflects the intensity mapping. The typical voltage and current were kept constant at 40 kV and 15 mA, respectively.

3.2.3. Fourier transform infrared (FTIR) spectroscopy

Fourier transform infrared spectroscopy (FTIR; Nicolet iS5; THERMO Scientific, Waltham, MA) with a scan rate of 4 cm^{-1} in the spectrum range of 400–4000 cm^{-1} was used for the identification of functional groups grafting on the additives.

3.2.4. X-ray photoelectron spectroscopy (XPS)

X-ray photoelectron spectroscopy (XPS, Thermo Fisher Scientific, Waltham, MA) was adopted to examine the chemical structure or the chemical states of the constituent elements present in the oleic acid-modified LaF_3 nanoparticles and the binding energy associated with different chemical bonds and related compounds.

3.3. Formulation of nanolubricants

In the formulation of nanolubricants, a calculated amount of nanoadditives was added to all base oils based on the weight percentage. First, 40 ml of base oils were weighted using an electronic balance machine (GR 202; A&D Private Ltd., Japan), having an accuracy of 0.01 mg. Based on the weight of the base oil, the required concentrations of additives were measured. The nanoadditives at different concentrations (0.025–0.15 wt.%) were added into all base oils and mixed with a magnetic stirrer (IKA, HS4, Germany) for 15 min at room temperature, followed by ultra- sonication for 1 h to obtain thoroughly dispersed nanolubricants.

3.4. Rheological investigation

Rheological analysis of all plain PAOs was carried out on an Anton Paar MCR 702 rheometer with cone-plate geometry (plate diameter = 50 mm, cone angle = 1˚, and the gap between the plates = 0.1 mm). The shear rate sweep tests were carried out at a shear rate range of 0.01-100 s^{-1} to determine the flow behavior of both oils. The frequency sweep tests were conducted in oscillation mode at a constant shear strain of 0.05 with the change in frequency from 0.1 to 100 rad/s to determine the viscoelastic behavior of oils. Both types of rheological tests were executed at a fixed temperature of 75℃. Rheological tests were performed thrice for both PAOs to ascertain the repeatability of the results.

3.5. Tribological experimentation

PAOs have acquired rapid admissibility as high-performance base oils in many applications, such as industrial bearing, automobile components as an engine lubricant and gear oil, turbine oil, compressor, and pump oil, automatic transmission oil, hydraulic oil etc. Most of these mechanical parts are encountered with various loads, speeds, and motion at the contacting surface of the rubbing pairs. Hence, selecting the best tribometer that simulates the real-world application becomes essential. Therefore, different tribometers were used in the present study to estimate the tribological performance of nanolubricants. The details of the tribometer are as follows:

3.5.1. Four-ball tribometer

The Four-ball tester is one of the most important tribometers for measuring the extreme pressure (EP) properties and wear prevention characteristics of lubricating oils under sliding contact. The four-ball method is set apart from other friction and wear tests by the unique arrangement of four steel test balls clamped together in the form of a tetrahedron. In a four-ball tribometer, all test balls are submerged in lubricating oil. Therefore, it is suitable to assess the tribological properties of lubricating oils under submerged lubrication conditions. Because of the steel balls used in the tests, the four-ball tribometer is specifically applicable for sliding steel-on-steel applications such as ball bearings, gears, automotive applications, etc. In the present study, the anti-wear and extreme pressure properties of nanolubricants have been evaluated using a four-ball tribometer (manufactured by Ducom Instrument Pvt. Ltd., Bengaluru, India) as per ASTM D4172 [122] and D2873 [123] standards, respectively. **Table 3.4** describes the details of test parameters according to ASTM. The high chromium alloy steel (AISI 52100) balls were used in the test. The diameter of the test ball was 12.7 mm, and the hardness was in the range of 59–61 HRC. Before the beginning of the test, steel balls, ball pot, collet, and splash guard were thoroughly cleaned with acetone. The schematic diagram of the four-ball tribometer is shown in **Figure 3.2**. The lower three balls were stationary in the ball pot, and the upper ball is mounted in the collet, which rotates against three lower balls with the assistance of a motor through a spindle. The coefficient of friction (COF) and frictional force was recorded in a computer attached to the tribometer through the controller unit. Extreme pressure (EP) tests were accomplished to verify the sustainability of nanolubricants under higher loading conditions in terms of pre-seizer load and seizer load. All experiments were executed three times to ensure repeatability.

Table 3.4: Summary of test parameters as per ASTM standard

Standards	Speed (rpm)	Time (sec)	Temperature (°C)	Load (Kgf)
ASTM D4172 ASTM D2266 (Anti-wear test)	1200 ± 60	3600 ± 1	75 ± 2	40 ± 0.2
ASTM D2873 ASTM D2596 (Extreme-pressure test)	1760 ± 40	10 ± 0.2 (At each load)	27 ± 8	6, 8, 10, 13, 16, 20, 24, 31, 40, 50, 63, 80, 100, 126, 160, 200, 250, 315, 400, 500, 620, 800

The ball-on-ball configuration is a point contact type geometry between the test balls in four-ball tester at the beginning of the experiment. The maximum contact pressure (P_{max}) developed between the contact point was found to be 3.4 GPa and the detailed calculations for P_{max} is illustrated in **Appendix-A**. The diameter of worn scars developed on three stationary balls during each test was measured by image acquisition. Further, the detailed calculations of the wear volume of steel balls are presented in **Appendix B**.

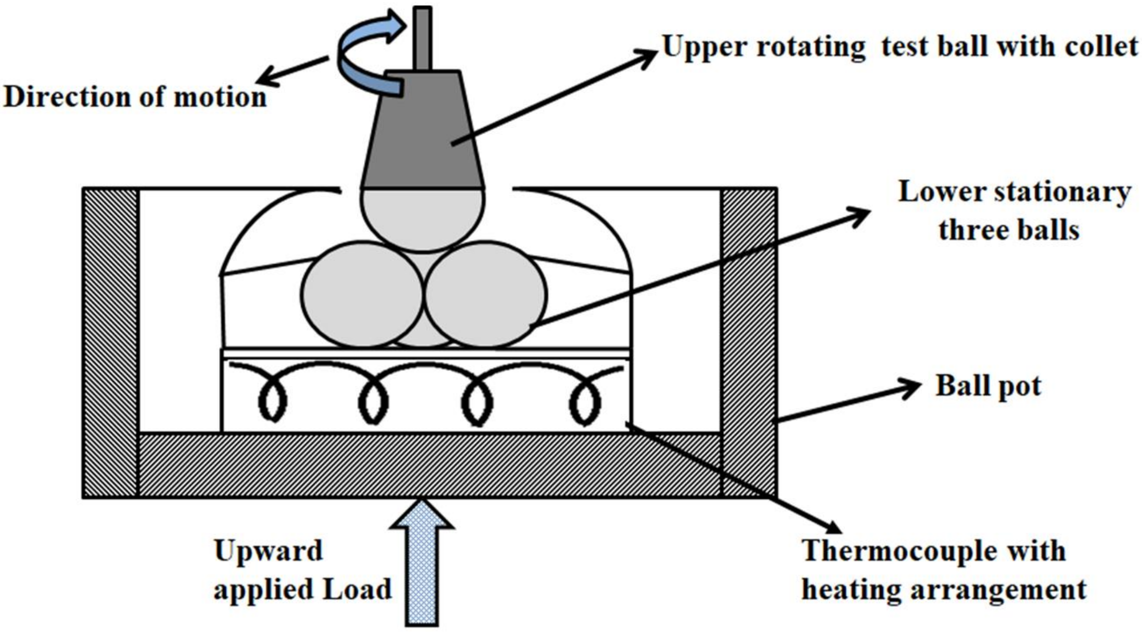

Figure 3.2: Schematic diagram of the four-ball tribometer

The minimum film thickness was calculated as per Hamrock and Dowson's equation [124] by assuming hard elastohydrodynamic lubrication. The calculated minimum film thickness for PAO 4, PAO 6, PAO 40, and PAO 100 was 14.34 nm, 21.27 nm, 151.6 nm, and 335.7 nm, respectively. Furthermore, the film thickness ratio (λ) was also determined to estimate the lubrication regimes. The computed values of λ were 0.051, 0.075, 0.533, and 1.18 for PAO 4, PAO 6, PAO 40, and PAO 100, respectively. From the theory of fundamentals of fluid film lubrication proposed by Hamrock et al.[125]. It was found that the operating lubrication regime was in boundary lubrication for PAO 4, PAO 6, and PAO 40 because λ is less than 1. however, it was mixed or partial lubrication in the case of PAO 100. The detailed calculations of h_{min} and λ are presented in **Appendix C**.

3.5.2. High-frequency linear-oscillation tribometer (SRV 5)

In mechanical components, many practical situations in which rubbing pairs undergo reciprocating/sliding motion, e.g., piston-cylinder arrangements, roller bearings, cam-follower, etc. A popular tribometer to determine the ability of lubricating oil to protect against wear and coefficient of friction is the SRV test rig. This test rig is best suited for rubbing pairs operated under starved lubrication conditions. In the present study, a high-frequency linear-oscillation tribometer (SRV 5; Optimol Instrument, Munich, Germany) was used to conduct tribological testing. Tribological experimentations were performed as per the ASTM D6425 standard. **Table 3.5** reports the test parameters and arrangement of the specimens. The ball-on-disc type geometry used in SRV 5 tribo testing validates the point contact between the mating pairs, causing Hertzian contact stress. The computed value of maximum contact pressure (P_{max}) between the mating pairs was 1.73 GPa, 2.74 GPa, and 3.14 GPa for a corresponding load of 50 N, 200 N, and 300 N, respectively. The detailed calculation for (P_{max}) is provided in **Appendix A**. Both the mating specimens were made from AISI 52100 high chromium-bearing steel. The diameter of the ball specimen was 10 mm, and microhardness was 60 ± 2 HRC. The disc specimen had a thickness of 7.85±0.1 mm and diameter of 24±0.5 mm. The hardness was 62 ± 1 HRC. In the test rig, the disc was mounted on a holder called the lower test specimen, while the test ball was loaded vertically with the aid of a load rod, called an upper test specimen. Before starting the experiments, 0.3 mL of lubricant was applied to the disc specimen at the contact area, which remained stationary throughout the test duration. The test ball oscillates against the disc with the assistance of an oscillation drive rod. The coefficient of friction (COF) for test duration was recorded in the computer through the data acquisition system attached to the test rig. The schematic diagram of the SRV 5 tribometer is portrayed in **Figure 3.3**. Figure 3.3 (a) represents the experimental set-up and the detailed arrangement of a ball on disc and load application. While Figure 3.3 (b) demonstrates a typical wear scar formation on the test specimens and the quantification of various parameters to calculate the wear volume. The planimetric wear (Wq) of the disc was acquired across the wear track via profilometric measurements (Hommeltester, Fa. Hommel, Hanau, Germany). After the test, the radius of the steel ball (R^*) was measured by a profilometer, and estimated the wear volume (WV) of the ball and disc. Further, the detailed calculations for estimating the wear volume of steel ball and disc are presented in **Appendix B**.

Hamrock and Dowson equation (**Appendix C**) was used for the theoretical estimation of the h_{min}. The calculated minimum film thickness (h_{min}) for PAO 4, PAO 6, PAO 100, and PPG 2000 was 4.71 nm, 6.23 nm, 96.7 nm, and 32.9 nm, respectively. Furthermore, the computed thickness ratio (λ) for PAO 4, PAO 6, PAO 100, and PPG 2000 was 0.114, 0.153, 2.35, and 0.779, respectively. It was observed that for PAO 4, PAO 6, and PPG 2000, the λ ratio was under unity, which means that the lubrication occurred in the boundary lubrication regime. However, in the case of PAO 100, the calculated value of λ was greater than unity, which is the potential evidence of a mixed or partial lubrication regime.

Table 3.5: Summary of test parameters as per ASTM D6425

Parameters	Value
Configuration	Ball-on-disc
Test ball	52100 steel; Hardness: 60±2 HRC; Surface roughness: Ra 0.025µm ± 0.005; Diameter =10 mm
Disc	52100 steel; Hardness: 62±1 HRC; Surface roughness: 0.035µm<Ra<0.050µm; Diameter =24 mm± 0.5 mm; Thickness =7.85 mm± 0.1 mm
Frequency (Hz)	50
Stroke (mm)	1
Temperature (ºC)	50, 80
Load (N)	50, 200, 300
Test duration (h)	2
Lubricant quantity (mL)	0.3
Environment	Laboratory air (Relative humidity 35-50%)

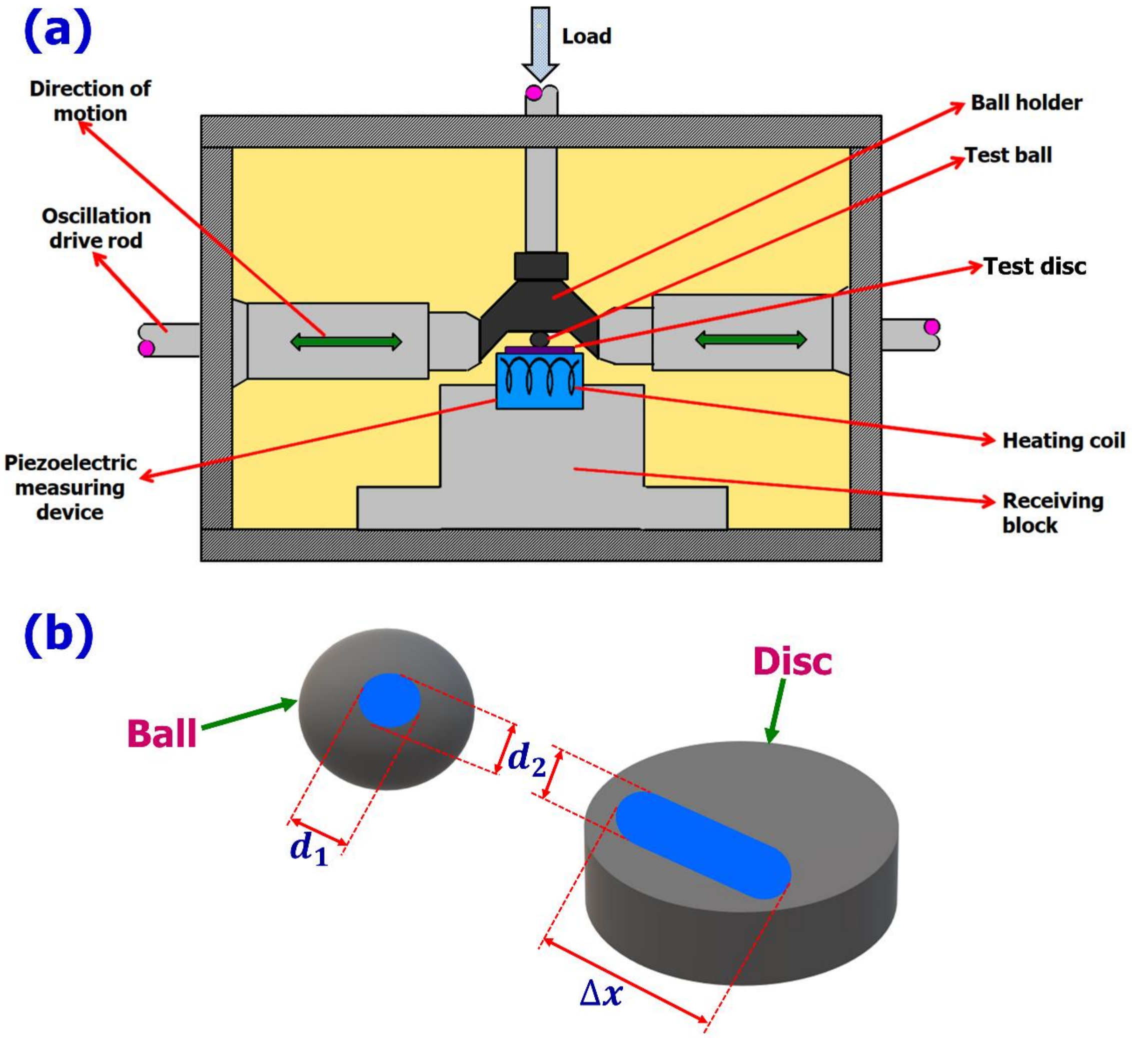

Figure 3.3: The schematic diagram of (a) SRV 5 test rig (b) wear scar of ball and disc and quantification of various parameters

3.5.3. Ball-on-disc tribometer

Pin-in-disc/ ball-on-disc tribometers are probably the most known and extensively used devices that simulate the tribo-contact situation for continuous sliding in a particular machine. This tribometer evaluates lubricants for a specific application and qualifies lubricants for the established criteria. The pin-on-disc/ball-on-disc tribometer is generally adopted to investigate the influence of variation in various parameters such as load, velocity, sliding distance, and temperature on friction and wear. A tribometer (Ducom Instrument Pvt. Ltd, India) with a "ball-on-disc" type arrangement was employed to perform the experiments. A high chrome-bearing steel ball (AISI 51200) with a diameter of 10 mm and hardness 59-61 HRC was used as an upper sample held stationary throughout the test duration. The lower sample, i.e., disc, is made of hardened steel (EN 31), having a hardness of 60 ± 2 HRC was mounted on a rotary drive. The disc had a thickness of 8 mm and a diameter of 165 mm. The friction surface of the disc was polished with 800, 1000, and 1200 grade emery paper, followed by acetone cleaning. The average roughness (R_a) of the disc and the ball were 0.202 μm and 0.201 μm, respectively. The "ball on disc" type configuration confirms the point contact at the mating surface at the beginning of the test. The calculated Hertz pressures were 1.7, 1.99, and 2.14 GPa, corresponding to 50, 80, and 100 N normal applied loads, respectively (**Appendix A**). Before the commencement of experimentations, 2 mL of lubricant was dispersed carefully on the track of the disc to preserve boundary/mixed lubrication conditions. All the experiments were carried out at room temperature for the total sliding distance of 3000 m and track diameter of 80 mm. All tests were carried out three times to ascertain the replicability. The friction force was automatically recorded in the computer through the data acquisition system of the tribo machine. The coefficient of friction (COF) was calculated by normalizing the frictional force by dividing it with applied load. The specific wear rate was calculated by assuming negligible disc wear compared to the ball in "ball on disc" type arrangement. The calculations for estimating the specific wear rate steel ball and disc are presented in **Appendix B**.

3.6. Synthesis of PAO 100-based grease

In the present study, PAO 100 based greases were synthesized using PAO 100 as base oil and 12–lithium hydroxystearate metallic soap as a thickener. The grease samples were prepared using a 12–hydroxystearic acid and lithium hydroxide monohydrate by in-situ saponification reaction. The 12–hydroxystearic acid and lithium hydroxide monohydrate were procured from Tokyo Chemicals Industry Co. Ltd. and Spectrochem Pvt. Ltd., respectively. The soap concentration was fixed at 14 wt.%. Batches of 250 g grease samples were prepared, so it required 35 g of 12–lithium hydroxystearate. Therefore, the detailed calculation of the stoichiometric amount of 12–hydroxystearic acid and lithium hydroxide monohydrate was required to formulate a 250 g sample of grease as presented in **Appendix D**.

Both nanoadditives (MWCNTs and LaF_3) were individually dispersed into PAO 100 at different concentrations in the range between 0.025–0.15 wt.%. A measured quantity of nanoparticles was dispersed into PAO 100 using a magnetic stirrer (IKA, C–MAG HS4 digital) at room temperature for 30 min. For homogenous dispersion of nanoadditives in the PAO 100, it was kept in an ultrasonication bath (Antech, GT–1730QTS) at room temperature for 1 h. Overhead mechanical stirrer (Remi Elektrotechnik Ltd, 8000 rpm) appended with a square-edged anchor impeller was used to stir the solution. 12–hydroxystearic acid was added slowly into the mixture, stirred continuously at 200±10 rpm, and heated at 90±2 °C. In parallel, lithium hydroxide monohydrate was dissolved homogeneously in distilled water and added dropwise to the mixture as soon as 12–hydroxystearic acid started to melt, and a waxy transformation occurred. The mixture was allowed to stir at 300±10 rpm at a temperature of 180±2 °C for two hours, followed by cooling at room temperature for 24 h.

3.7. Characterization of grease

National Lubricating Grease Institute (NLGI), in association with the American Society of Testing Materials (ASTM) has standardized the test specifications and procedures for testing the grease. The physicochemical properties (i.e., consistency and drop point) and tribological properties of greases were assessed as per ASTM standards.

3.7.1. Characterization of physicochemical properties of greases

3.7.1.1. Consistency

The term consistency refers to the thinness or thickness of grease that affects the flowability of grease. The type and concentration of thickener have the most significant influence on the consistency, whereas the viscosity of the base oil has a minor impact. In the present study, the consistency of all grease samples was measured using the cone penetrometer (Khusboo Scientific Instrument Pvt. Ltd., India) as per the ASTM D1403 standard. When the quantity of grease samples is limited, one–half ($^1/_2$) or one–quarter ($^1/_4$) scale cone equipment is employed to assess the consistency of the grease. This test determines the NLGI consistency number of the grease by evaluating its unworked and worked penetration depth. The test conditions for unworked and worked penetration measurements are the same as stated in **Table 3.6**. If the penetration measurements are obtained with $^1/_2$ scale or $^1/_4$ scale, the cone penetrometer must be converted to full scale using the following equations.

For $^1/_2$ scale, $$P = 2p' + 5 \tag{3.1}$$

For $^1/_4$ scale, $$P = 3.75p'' + 24 \tag{3.2}$$

Where;

P= cone penetration by test method D217

p'= cone penetration by ½ scale equipment

p'' = cone penetration by ¼ scale equipment

In unworked penetration, the measurements are obtained on the undisturbed grease structure. In worked penetration, a grease worker is used to shear the grease structure. Based on worked penetration depth measurements, the NLGI assigns a consistency number to the grease. The NLGI consistency number categorizes the hardness of the grease in the range of 85 (NLGI 6) to 475. (NLGI 000). NLGI 000 refers to the fluid, while NLGI 6 corresponds to hard grease. **Table 3.7** summarizes the framework of NLGI classification.

Table 3.6: Test conditions used for the determination of the grease consistency

ASTM Standard	Type of scale	Weight of cone assembly, g	Quantity of grease, g	Duration, s	Temperature, °C
D217	Full scale	150±0.1	400	5±0.1	25±0.5
D1403	Half scale	37.5±0.050	-	5±0.1	25±0.5
	Quarter scale	9.38±0.025	-	5±0.1	25±0.5

Table 3.7: Grades of grease classified according to NLGI (ASTM D217)

NLGI grade	Work penetration depth after 60 strokes at 25 °C (0.1 mm)	Appearance
000	445-475	Fluid
00	400-430	Semi-fluid
0	355-385	Very soft
1	310-340	Soft
2	265-295	Normal
3	220-250	Firm
4	175-205	Very firm
5	130-160	Hard
6	85-115	Very hard

3.7.1.2. Drop point

The drop point is also a critical property to evaluate the performance of the grease. When the grease is heated, it softens and turns its phase from semi-solid to liquid. The drop point is the temperature at which grease transforms its phase from semi-solid to liquid. The drop point is referred to as the "melting point" of the grease. At this temperature, the thickener faded its property to constrain base oil within its fibrous network. Some non–soap-based grease does not melt with the increment of temperature and can be stable up to the thickener or base oil decomposition temperature. Therefore, these greases do not show a drop point and are preferably used for bakery ovens. The drop point of grease samples was evaluated using the drop point apparatus (Khusboo Scientific Instrument Pvt. Ltd., India) as per the ASTM D566 standard.

In this test, the grease was heated under prescribed conditions. When the first drop of oil was detached from the grease matrix and fell in the bottom of the tube, that temperature is referred to as "drop point," which was an average of two thermometer readings. In this test method, the bath temperature is limited to 288 °C, and the drop point of grease was determined over a wide range of temperatures through the ASTM D2265 standard. The thickener used in the grease formulation affects the drop point and the maximum applicable working temperature of the grease.

3.7.2. Characterization of tribological properties of grease using four-ball tester

A four-ball tribometer (manufactured by Ducom Instrument Pvt. Ltd., Bengaluru, India) was used to assess the AW and EP properties of grease samples as per ASTM D2266 and ASTM D2596 standards, respectively. The description of the four-ball tribometer and test procedure are explained in **Section 3.5.1**. Further, the detailed calculations of maximum contact pressure and the wear volume of steel balls are illustrated in **Appendix A** and **Appendix B**.

3.8. Characterization of worn surfaces

3.8.1. Scanning electron microscope (SEM) and Energy-dispersive X-ray spectroscopy (EDS)

To investigate the wear mechanism and morphologies of the worn surface of the tested samples, scanning electron microscopy (SEM; EVO 15/18; CARL, Germany) was employed. The operating voltage was kept constant at 20 kV, and the working distance between the electron gun and specimen was maintained in the range between 10–10.5 mm. The chemical elemental analysis of worn surfaces was carried out using energy-dispersive x-ray spectroscopy ((EDS; 51N1000; Oxford Instrument Nanoanalysis, UK), attached with SEM.

3.8.2. X-ray photoelectron spectroscopy (XPS)

X-ray photoelectron microscopy (XPS; Thermo Fisher Scientific, Waltham, MA) having Al Kα radiation X-ray source was used to investigate the surface chemistry of tribo-film developed on the worn surfaces. XPS is typically accomplished by exciting the surface of a sample with mono-energetic Al kα x-rays causing photoelectrons to be emitted from the sample surface. The electron emitted from the electron shell of an atom exhibits characteristics energy levels, unveiling the composition of chemical elements in the sample being examined. The XPS operates under ultra-high vacuum (10^{-9} bar).

3.8.3. Scanning probe microscope (SPM)

A scanning probe microscope (SPM; NT-MDT Services & Logistic Ltd, Russia) was performed for topographical characterization of worn surfaces of tested balls. Primarily, the worn surface was cleaned with acetone, and the roughness of the worn area of 20×20 μm and 60×60 μm was measured with a silicon nitride cantilever (tip radius:10 nm) in a tapping mode at a scanning rate of 0.5 Hz.

3.9. Summary of the chapter

This chapter discusses the methodology used for synthesizing nanoadditives, greases, and tribo-testing, basic calculations for tribological parameters. In addition, the chapter provides a brief overview of the analytical tools used in this work.